Crystal Structures and Properties of Nylon Polymers from Theory

Siddharth Dasgupta,*,† Willis B. Hammond,‡ and William A. Goddard III*,†

Contribution from the Materials and Process Simulation Center (CN 1401), Beckman Institute (139-74), Division of Chemistry and Chemical Engineering (CN 8966), California Institute of Technology, Pasadena, California 91125, and AlliedSignal Inc., Morristown, New Jersey 07962

Received December 22, 1994. Revised Manuscript Received July 19, 1996[⊗]

Abstract: A complete force field (MSXX) for simulation of all nylon polymers is derived from *ab initio* quantum calculations. Special emphasis is given to the accuracy of the hydrogen bond potential for the amide unit and the torsional potential between the peptide and alkane fragments. The MSXX force field was used to predict the structures, moduli, and detailed geometries of all nine nylons for which there are experimental crystal data plus one other. For nylon-(2*n*) with $2n \leq 6$, the α crystal structure (with all-trans CH_2 chains nearly coplanar with the hydrogen bonding plane) is more stable, while for $2n > 6$, γ (with the alkane plane twisted by 70°) is more stable. This change results from the increased importance of methylene packing interactions over H bonds for larger 2*n*. We find the highest Young's modulus for nylon-7.

1. Introduction

Nylon polymers consist of polyethylene segments $(CH_2)_n$ separated by peptide units (NH−CO) which are either parallel or antiparallel:

$$\text{nylon-}n\text{:}\quad -[-(\text{NH}-\text{CO})-(-\text{CH}_2)_{n-1}-]- \qquad (1)$$

$$\text{nylon}-m,n\text{:}\quad -[-(\text{NH}-\text{CO})-(\text{CH}_2)_{n-2}-(\text{CO}-\text{NH})-(\text{CH}_2)_m-]- \qquad (2)$$

These peptide units provide hydrogen bonding between polymer chains (see Figure 1), giving nylon some of its unique properties. In contrast to other highly crystalline polymers like polyethylene, nylon polymers can have their degree of crystallinity controlled over a wide range. It has a unique combination of stiffness, toughness, lubricity, and resistance to abrasion, fatigue, and temperature that makes it one of the most versatile thermoplastics in use today. By changing the amide density, one can modify such properties as the melting point, moduli, low-temperature impact strength, moisture absorption, and chemical resistance to metal salts and acids. The two largest volume nylon polymers are nylon-6 and nylon-6,6 which are widely used for carpets and garments. Nylon-11 and nylon-12 are mainly used in tubing extrusion, cable jacketing, injection molding, and coating of metal objects.

Despite the industrial importance of nylon polymers, there remain considerable uncertainties about the crystal structures, moduli, and other properties of these systems. Nylon polymers tend to be partially crystalline, but reliable experimental information about the ordered regions is difficult to obtain. Generic force fields (developed without special emphasis on nylon moieties) tend to have incorrect torsional preferences for the small-molecule analogs of the nylons. Additionally, the room temperature dynamics indicates that the crystal structures are metastable and distort severely. Consequently, we have used *ab initio* quantum chemistry (QC) to develop the new MSXX force field (FF) suitable for all forms of nylon polymers, including crystals and amorphous and partially crystalline systems. This MSXX FF is applied here to all nine nylon polymers for which there is structural information and to one other.

Since the unique structural and thermomechanical properties of nylon polymers are dominated by the hydrogen bonds in these polyamides, we paid careful attention to the description of hydrogen bonding. QC was used to determine the hydrogen-bonding potentials, an approach that should be useful for all hydrogen-bonded systems (including peptides and DNA). The regularities of nylon polymers make them ideal for validating the hydrogen bond potential.

Section 2 derives the MSXX FF for nylon polymers. Section 3 discusses the various nylon crystals and the properties predicted with the MSXX FF.

2. MSXX Force Field

2.1. Hydrogen Bond Potential. 2.1.1. Calculational Details. All *ab initio* calculations were done using the Gaussian92 suite of programs[1] while all molecular mechanics calculations were done with PolyGraf[2] modified at Caltech. For all the MM calculations, the convergence criteria used were 0.01 kcal/(mol Å) for atom rms forces and 0.1 kcal/(mol Å) rms cell forces. For the calculation of the zero point energy of the crystal structures, we chose *n* equally spaced points along each reciprocal lattice vector. All phonons at all the $n = 3$ points were treated as Einstein oscillators for calculating the partition function. Usually, at $n = 3$, the zero point energies were converged.

To derive FF parameters for simulation of nylons, we studied various model systems using *ab initio* quantum chemistry (QC) calculations at two levels: (i) MP2/6-31G** Møller−Plesset perturbation theory for electron correlation using a valence double-ζ basis set with polarization functions on all atoms and (ii) HF/6-31G** Hartree−Fock (uncorrelated) with the same basis set. The binding energy of complexes will generally be overestimated due to basis set superposition error (BSSE).

* To whom correspondence should be addressed. E-mail: sdg@wag.caltech.edu, whammond@coin.csnet.net, and wag@wag.caltech.edu.
† California Institute of Technology.
‡ Allied Signal Inc.
⊗ Abstract published in *Advance ACS Abstracts,* December 1, 1996.

(1) Frisch, M. J.; et al. *Gaussian 92*; Gaussian Inc.: Pittsburgh, PA, 1992.
(2) Biograf/Polygraf from Molecular Simulations Inc., San Diego, CA.

S0002-7863(94)04125-9 CCC: $12.00

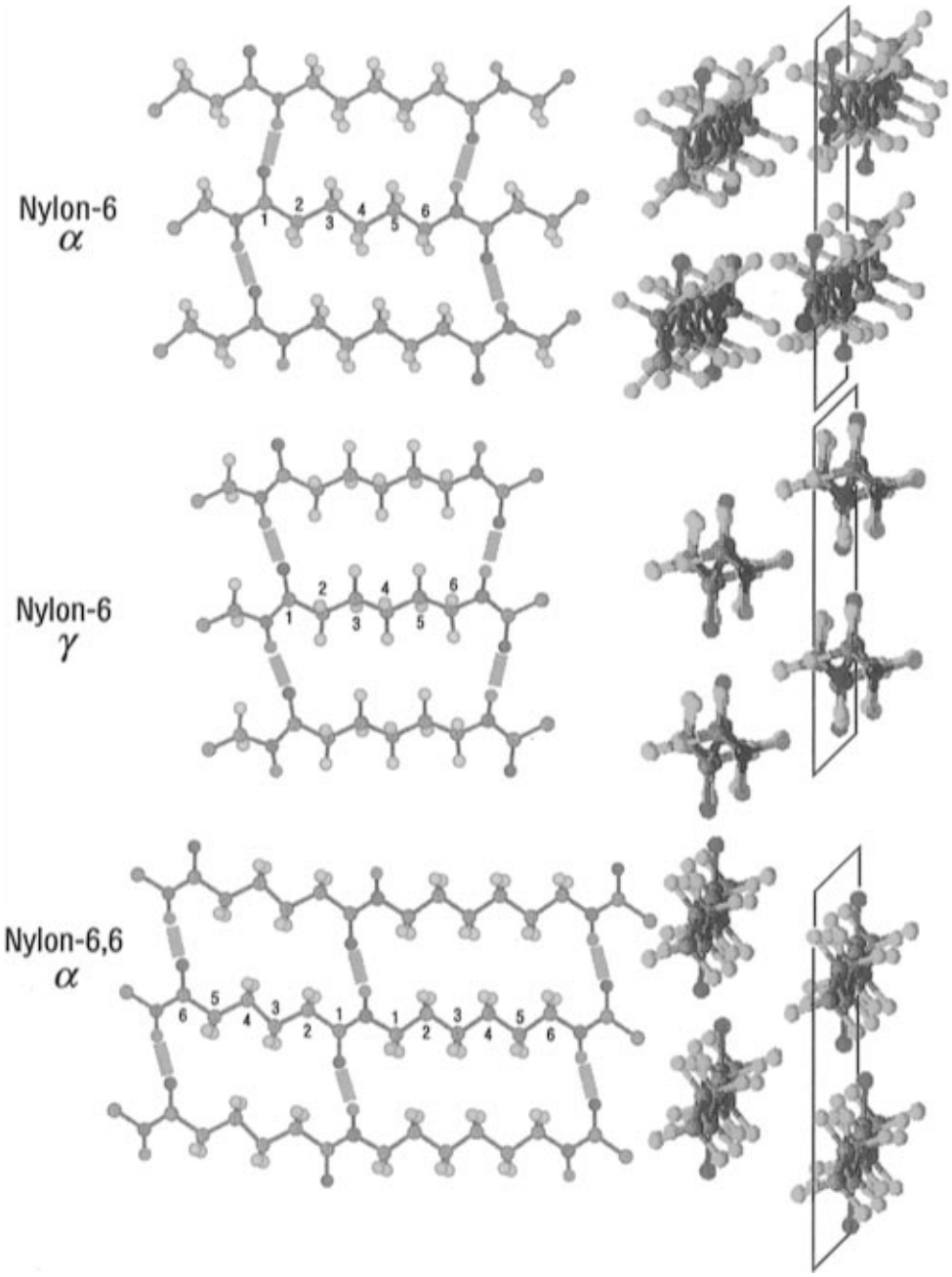

Figure 1. Structures of the α and γ forms of nylon-6 and of nylon-6,6. The left side shows the view of the hydrogen-bonding planes, and the right side shows the view down the chain axis. For the α form of nylon-6, the adjacent chains are antiparallel and the hydrogen bonding is between adjacent chains within the *same sheet* (bisecting the CH_2 angles). For the γ form of nylon-6, the chains are parallel and the hydrogen-bonding is between chains in *adjacent sheets*. In nylon-6,6, the chains have no directionality.

Consequently, we correct BSSE using the counterpoise method[3] which uses all basis functions for the complex in calculating the energy of the constituent molecules. Since the complex can use only the *unoccupied* orbitals of the partner, the counterpoise calculation overcorrects for the BSSE by about 5−10% of the total BSSE correction.[4]

The new hydrogen bond potential is derived from calculations of the formamide dimer, Figure 2. Subtracting electrostatic interactions (based on fixed point charges extracted from QC on the monomers) leads to a new form of the short-range hydrogen bond potential. Since experimental data are unavailable for this dimer,[5] we tested it by calculations of the water−formamide and formaldehyde−formamide complexes, where microwave gas phase structure determinations have been reported[6] following *ab initio* calculations.[7]

2.1.2. Water−Formamide Complex. In order to determine whether the 6-31G** basis is adequate, we also considered the more complete TZ2P^{++} basis (which contains three sets of valence s and p functions instead of two, plus two sets of polarization functions rather than one, plus a set of diffuse function).

For the water−formamide complex, we calculated the structure and the binding energies using MP2 with both basis

(3) Boys, S. F.; Bernardi, F.; *Mol. Phys.* **1970**, *19*, 553.
(4) Yang, J.; Kestner, N. R. *J. Phys. Chem.* **1991**, *95*, 9214−9220, 9221−9230.
(5) It would probably exhibit a cyclic structure with two hydrogen bonds like the formamide−water and formamide−methanol complexes. For the nylons of interest to this study, the orientation of the two formamide dimers, Figure 2, is different than would be present in the cyclic dimer.
(6) Lovas, F. J.; Suenram, R. D.; Fraser, G. T.; Gillies, C. W.; Zozom, J. *J. Chem. Phys.* **1988**, *88*, 722.
(7) Jasien, P. G.; Stevens, W. J.; *J. Chem. Phys.* **1986**, *84*, 3271−3277.

Table 1. Geometric and Energetic Quantities[a] for the Formamide−H_2O Complex (See Figure 2 for Notation)

structure	method	basis	binding energy[b] CP	binding energy[b] No CP	OH:::O r_1	NH:::O r_2	H:::OC θ_1	OH:::O θ_2	HO:::H θ_3	NH:::O θ_4	out-of-plane Φ	rotational constants A	B	C
opt	exptl	exptl[c]			2.03	1.99	107.1	143.3			15.3	11.228	4.587	3.25
monomer	MP2	TZ2P^{++} [d]	8.244	9.648	1.91	2.08	102.3	151.7	79.8	137.2	42.4	11.141	4.658	3.30
opt	MP2	6-31G** [e]	8.411		1.93	2.01	105.6	151.4	79.5	140.4	65.3	11.015	4.693	3.32
monomer	MP2	6-31G** [f]	7.798	12.397	1.96	2.05	105.9	151.5	79.3	139.7	65.9	11.003	4.628	3.28
opt	HF	DZP[g]	7.9		2.06	2.16	110.1	143.3	83.7	138.6	0.0[g]	11.304	4.382	3.15

[a] Units: energy, kcal/mol; distances, Å; angles, deg. [b] CP is the counterpoise correction. [c] Reference 6. [d] This is the highest level of calculation. The structure of the monomer was fully optimized at the MP2 level using the TZ2P^{++} basis set. [e] The structure of the complex was fully optimized at the MP2 level but with the 6-31G** basis set. [f] The geometry of each monomer was kept fixed at the geometry for an isolated monomer as calculated using MP2/6-31G**. [g] Reference 7. This calculation was restricted to a planar geometry. The 1s core electrons on the heavy atoms were replaced by core effective potentials (CEP) which reduces BSSE.

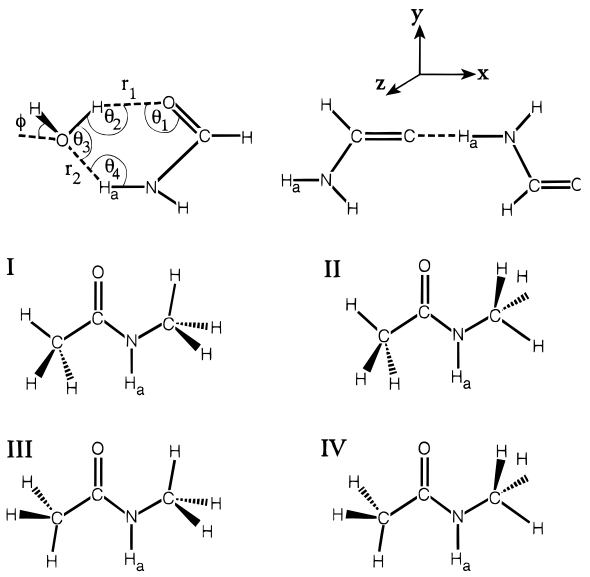

Figure 2. Molecular structures.

sets. The energies, geometries, and rotational constants are compared with the experiment[6] in Table 1. The 6-31G** basis leads to a bond energy just 0.17 kcal/mol too high (2%) and slight changes in the geometry (0.02−0.07 Å in bond distances, up to 3° in angles). Compared to experiment, we see differences of about 0.1 Å (5%) in the bond distances, 5−8° in the bond angles, and a significant discrepancy in the tilt of the water plane with respect to the formamide plane: calculated, 65.3° for MP2/6-31G** and 42.4° for MP2/TZ2P^{++}; experimental, 15.3°. Such discrepancies are expected because experiment measures the vibrationally averaged structure over the double-minimum potential which has an interconversion barrier of only 0.11 kcal/mol (35 cm^{-1}).

The internal geometry was optimized at each level of calculation for all monomers. In many previous dimer calculations, the geometries of the constituent molecules were frozen and only the intermolecular parameters allowed to optimize. This constraint is not too restrictive for the final geometries and energies of hydrogen-bonded complexes, as borne out by our calculations for the formamide−water duplex. Here we also allowed the internal geometries to optimize (at the MP2/6-31G** level). The data, Table 1, show that the binding energy changes by 0.61 kcal/mol or 7.3% while the change in the intermolecular geometry is 0.03−0.04 Å (1.5−2%).

Table 2 shows that the monomer geometries are described quite accurately at the MP2 level with both basis sets (bonds within 0.018 and 0.002 Å and angles within 1.8° and 1.1° for 6-31G** and TZ2P, respectively). The calculated dipole moments for the monomers agree well with the experimental values. Since hydrogen bonding is dominated by the electrostatic interactions, it is important to ensure that the long-range electrostatics is accurately described. This is evidenced by the accuracy in the calculated dipole moment (within 0.26 D for 6-31G** and 0.14 D for TZ2P).

Table 2. Monomer Geometries[a]

	source	exptl[b]	MP2/TZ2P^{++}	MP2/6-31G**
H_2O	HO	0.957	0.960	0.961
	HOH	104.5	104.35	103.8
	dipole	1.85	1.92	2.11
formamide	C−N	1.342	1.358	1.360
	C=O	1.219	1.218	1.223
	NH1	1.002	1.004	1.005
	NH2	1.002	1.002	1.002
	CH3	1.098	1.100	1.100
	CNH1	118.5	119.2	118.8
	CNH2	119.9	121.0	121.7
	OCH	122.6	122.6	123.1
	OCN	124.7	124.8	124.8
	dipole	3.73	3.87	3.78
formaldehyde	C=O	1.203		1.219
	C−H	1.099		1.099
	HCH	116.5		115.5
	OCH	121.7		122.2
	dipole	2.33		2.23

[a] Units: distances, Å; angles, deg; dipole, D. [b] Reference 49.

Calculations of the formamide−water complex have often assumed[7] a planar (C_s symmetry) structure; however, our calculations (*vide supra*) and experiment[6] both lead to a C_1 structure with the water plane tilted from the plane of the formamide molecule.

The geometrical parameters for the optimized complex agree well with experimental values. The calculated intermolecular parameters at the minimum in the potential energy surface are reported in Table 1 for both (i) the case with the monomer geometries frozen and (ii) the case where they are allowed to relax. While the calculated rotational constants are in very good agreement with the experimental results, there are a couple of significant differences. The water H to carbonyl O distance (r_1 in Table 1) is smaller than the water O to amide H distance (r_2 in Table 1) in all calculations ($r_1/r_2 = 0.918-0.956$) and is reversed from the experimental ratio ($r_1/r_2 = 1.020$). Optimizing the geometry of the monomers (at MP2/6-31G** level) in the complex reduces r_2 so that $r_1/r_2 = 0.960$. More significantly, the tilt of the water H−O−H plane is calculated to be much larger than deduced from the microwave spectrum. The geometry optimizations were started from the experimental structure (a tilt of 15.3°), but we find that this tilt increases to 65.3° for the fully optimized structure, 65.9° for the frozen monomer complex at the MP2/6-31G** level, and 42.4° with the larger basis set. This tilt orients the oxygen lone pair orbital of water to point toward the amide N−H bond, which should optimize the H bonding. Using the frozen monomer geometries, the calculated barrier to planarity for this complex is 0.109 kcal/

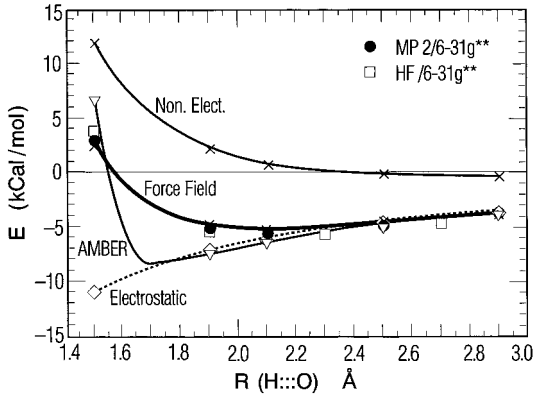

Figure 3. Binding energy for the coplanar formamide dimer in the direction of the collinear hydrogen bond. All energies are plotted on a relative scale where the energy of the system at a separation of 1000 Å is 0.0 kcal/mol. *Ab initio* calculations at the MP2 level of electron correlation used the 6-31G** double-ζ plus polarization basis set (with Gaussian 92).[1] [Hartree−Fock calculations are also reported for comparison.] At each level of calculation the geometry of each isolated monomer was optimized and kept rigid, forming the dimer, unless otherwise noted. We used the counterpoise method to correct for basis set superposition error (BSSE).[3] At the MP2/6-31G** level, this correction is less than 10%.[4] The FF calculations used a modified version of POLYGRAF[2] for each monomer. The electrostatic potential derived charges (using the CHELPG algorithm[22b]) were calculated from the MP2 wave function. These charges reproduce the experimental dipole moments well. The charges are used in the dimer without readjustments.

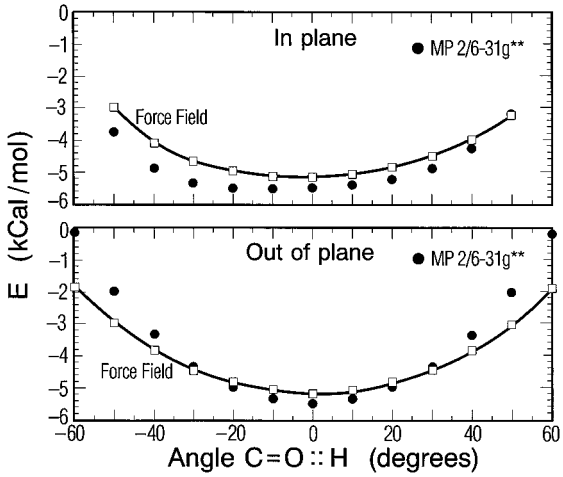

Figure 4. Binding energy for the formamide dimer. The energies are relative to zero energy at very large separation. (a, top) In the direction perpendicular to the hydrogen bond but in the molecular plane. This has been referred to as the "sliding" motion where the C═O and the H−N bonds are kept parallel to their original collinear geometry. The *x* axis is labeled by the regularly spaced changes in the angles while the concomitant change in the O:::H distance has not been labeled. (b, bottom) In the direction perpendicular to the plane of the formamides.

mol (at the MP2/TZ2P^{++} level) but without BSSE corrections. This barrier (35 cm^{-1}) between the double-welled minimum is well below the zero point energy (ZPE). Consequently, experiment is likely to find a vibrationally averaged structure close to planar structure despite a very nonplanar equilibrium structure. Similarly for glycine a nonplanar structure was calculated where a planar structure is inferred from experiment.[8]

The calculated complexation energy is 8.244 kcal/mol with the larger basis set and 7.798 kcal/mol with 6-31G**. Without correction for BSSE, these numbers are 9.648 and 12.397 kcal/mol, respectively. As expected, the larger basis set with diffuse functions has the smaller superposition error.

2.1.3. Formamide Dimer. For the formamide dimer, the noncyclic single hydrogen-bonded geometry shown in Figure 2 mimics the amide geometry of adjacent chains in nylons. Figure 3 shows the hydrogen bond interactions for the formamide dimer [MP2/6-31G** corrected for basis set superposition error (BSSE)]. The well depth is 5.18 kcal/mol at an O···H separation of 2.10 Å. HF calculations with BSSE correction lead to a well depth of 5.85 kcal/mol, and the O···H separation is 2.10 Å; this compares to 5.10 kcal/mol and 2.00 Å for similar calculations on the H_2O dimer.[9]

Keeping the C═O···H−N axes parallel (the *x* axis) and the peptide bonds coplanar (the *xy* plane), we see in Figure 4a that the potential for in-plane sliding (the *y* direction) is quite soft (this motion moves the proton past one of the sp^2 lone pairs of the carbonyl). Such parallel CO and HN bonds are relevant to nylons.

Displacement in the out-of-plane direction *z* results in a much stiffer potential (see Figure 4b), due to rapid loss of overlap with the lone pairs. Indeed, one could argue that charges should be centered on these lone pairs in order to properly describe the angular dependence of electrostatics. In the particular case of the carbonyl lone pairs, one would also have to model the anisotropy of the angular dependence in-plane vs out-of-plane, which requires a four-body term rather than the current simple two-body terms we use. Since we use only atom-centered charges for convenience in molecular dynamics, there is nothing additional to fit here and these comparisons serve as an overall test of the assumption that all potentials can be centered on the atoms and that the van der Waals (vdW) interactions can be described as sums of two-body terms.

2.1.4. H···O van der Waals Potential. At intermediate distances the strongly attractive behavior of hydrogen bonds is primarily due to electrostatic interactions, while at short distances, there are other effects including Pauli orthogonality, polarization, and London dispersion. We group these other effects together in a single vdW potential. We use the charge distribution of the isolated molecule to determine the long-range electrostatic interactions. From Figure 3 we see that this electrostatic potential nearly coincides with the total potential for $R > 2.5$ Å, but at shorter distances the electrostatic curve is too attractive. To determine the H···O vdW potential we start with the total QC potential, subtract the electrostatic potential, and subtract all vdW interactions *except* the H···O interaction. The resulting H···O vdW potential is strongly repulsive for short distances (due to orthogonalization of the orbitals arising from the Pauli principle) and slightly attractive at larger distances (the London dispersion forces resulting from instantaneous correlation of dipole fluctuations on the separate molecules).

The MP2 level of electron correlation describes the simultaneous fluctuations in the charges of molecules responsible for the London attraction; however, the 6-31G** basis set is not sufficient for an accurate description of these long-range attractive forces at larger distances. However, such larger basis sets have little effect on the bond energies and geometries near the equilibrium region. Consequently, we have adopted MP2/6-31G** as a practical level of calculation for systematic application to a wide variety of systems.

Given the numerical potential in Figure 3 from the *ab initio* calculations, it is useful to have an analytic form of the vdW energy for use in molecular dynamics studies. We find that an adequate description is given by the pure exponential form

(8) Frey, R. F.; Coffin, J.; Newton, S. Q.; Ramek, M.; Cheng, V. K. W.; Momany, F. A.; Schaefer, L. *J. Am. Chem. Soc.* **1992**, *114*, 5369−5377.
(9) Kollman, P. A. In *Methods of Electronic Structure Theory*, Schaefer, F., Ed.; Plenum Press: New York, 1977; Vol. 2, Chapter 3.

$$E_{\mathrm{vdW}}^{\mathrm{EXP}} = A \exp\left[-\frac{(R - R_e)}{C}\right] \tag{3a}$$

with $A = 0.028$ kcal/mol, $C = 0.251$ Å, and $R_e = 3.017$ Å. To describe the long-range attraction in the vdW potential, one can replace (3a) with the Morse function

$$E^{\mathrm{Morse}} = A\left\{\exp\left[\frac{-(R - R_e)}{C}\right] - 2\exp\left[\frac{-(R - R_e)}{2C}\right]\right\} \tag{3b}$$

However, for the cases considered here, (3b) leads to essentially the same results as (3a).

To test transferability of the new potential, we carried out similar MP2 calculations on the formamide−formaldehyde complex, leading to $R_{O\cdots H} = 2.10$ Å and $D = 3.72$ kcal/mol. Using the electrostatic potential for formamide and formaldehyde, we find values of $A = 0.029$ kcal/mol, $C = 0.251$ Å, and $R_e = 3.013$ Å, confirming the transferrability of (3a).

2.1.5. Comparison to Other H Bond Potentials. A variety of H bond potentials have been used for molecular dynamics simulations. The AMBER FF[10] describes hydrogen bonds as a combination of electrostatic forces plus a 10−12 Lennard-Jones potential, $E_{\mathrm{vdw}}^{\mathrm{amber}} = AR^{-12} - BR^{-10}$. The new version, AMBER2,[11] uses a combination of electrostatics and the normal 6−12 Lennard-Jones potential to describe H bonds. This uses charges based on the restrained electrostatic potential (RESP) scheme to fit the quantum mechanical wave functions.[12]

Exponential (3a) and Morse-like (3b) potentials have been proposed earlier (see ref 11 for compilation of various forms of H bond potentials in the literature). Damewood et al.[13] argue that one should retain the same form of the nonbonded potential for all atoms as this does not require decisions as to which atoms are special H-bonded atoms. They provided a method for using experimental (and/or *ab intio*) data to parametrize the H bond parameters using the standard vdW potentials for the other atoms. However, all these methods focus on the binding energy and equilibrium bond length of the H bond and not on the full potential energy curve.

Our method is distinct from all of these others since we calculate the full PES curve (in the directions that are especially important) and base our modeling potential on fitting the entire *ab initio* data.

2.2. Valence FF. For nylon the key FF parameters involve the peptide unit, and hence we used *N*-methylacetamide as the model for determining the valence FF.

Previous MP2/6-31G* calculations[14] on conformers **I**, **III**, and **IV**, Figure 2, indicated that conformer **III** is the lowest in energy, but that the other conformers have comparable energies (within 0.093 kcal/mol) with quite small barriers for interconversion (≤0.1 kcal/mol). Conformer **IV** was found to be the lowest[15] at the HF/6-31G* level. Structural and energy parameters are reported in Table 1S (Supporting Information).

At the MP2/6-31G** level, we find the same four low-lying conformers, all within 0.13 kcal/mol (Figure 2). However, we find that **I** has the lowest energy. At room temperature all conformers are expected to be significantly populated. Indeed, Mirkin and Krimm (MK)[15] used scaled frequencies from HF/4-31G* to show that all conformers are present in Ar and N_2 matrices [they were able to assign all the observed fundamental frequencies in the spectrum to proper normal modes].

We used the biased Hessian (BH) method[16] to optimize the valence FF parameters for *N*-methylacetamide on the basis of the normal mode description from HF/6-31G** and the vibrational frequencies from experiment. BH uses singular value decomposition (SVD)[17] to optimize the parameters in the FF with the constraints of fitting: (i) the given geometry (by obtaining zero forces), (ii) the normal mode eigenfunctions, and (iii) the experimental vibrational frequencies.

The FF is taken to have the form

$$E = E_{\mathrm{bond}} + E_{\mathrm{ang}} + E_{\mathrm{torsion}} + E_{\mathrm{inv}} + E_x + E_{\tau x} + E_{\mathrm{vdW}} + E_{\mathrm{Q}} \tag{4}$$

E_{bond} used Morse (5a) or Harmonic (5b) bond potentials

$$E_{\mathrm{bond}} = D_b[e^{-\alpha_b(R-R_b)} - 1]^2 \tag{5a}$$

$$E_{\mathrm{bond}} = (1/2)K_b(R - R_b)^2 \tag{5b}$$

where R is the length of the bond, R_b and D_b are the position and depth of the well, and $K_b = 2D_b\alpha_b^2$ is the force constant. E_{ang} uses

$$E_{\mathrm{ang}} = (1/2)C_\theta(\cos\theta - \cos\theta_e)^2 \tag{6}$$

where θ is the angle, θ_e is the equilibrium angle, and $K_\theta = C_\theta \sin^2\theta_e$ is the diagonal force constant. E_{torsion} is

$$E_{\mathrm{torsion}} = (1/2)\sum_{n=0}^{6} V_n \cos n\tau \tag{7}$$

where τ is the torsional angle ($\tau = 0$ for cis), and V_n is the barrier (energy of cis over trans). For sp^3-sp^3 single bonds, there are nine possible dihedral combinations. These nine terms are scaled by 1/9 so that the net barrier for rotation remains V_n. E_{inv} is

$$E_{\mathrm{inv}} = (1/2)C_i(\cos\psi - \cos\psi_i)^2 \tag{8}$$

Given an atom I bonded to exactly three other atoms, J, K, and L, ψ is the angle between the IL bond and the IJK plane and ψ_i is the equilibrium value ($\psi_i = 0$ corresponds to the planar configuration). Here the force constant is $K_\phi = C_i \sin^2\psi_i$ and the barrier to planarization is

$$V_{\mathrm{bar}}^{\mathrm{inv}} = (1/2)C_i(1 - \cos\psi_i)^2$$

There are three possible choices for L. To remove any biases, we sum over all three and multiple by 1/3.

For each angle term we use the bond−angle and bond−bond cross terms:

$$E_x = K_{r_1\theta}(r - r_e)(\cos\theta - \cos\theta_e) + K_{r_2\theta}(r - r_e)(\cos\theta - \cos\theta_e) + K_{r_1r_2}(r_1 - r_{1e})(r_2 - r_{2e}) + K_{\theta_1\theta_2}(\theta_1 - \theta_{1e})(\theta_2 - \theta_{2e}) \tag{9a}$$

We also include two-center angle−angle terms described by

(10) Weiner, S. J.; et al. *J. Am. Chem. Soc.* **1984**, *106*, 765.
(11) Cornell, W. D.; et al. *J. Am. Chem. Soc.* **1995**, *117*, 5179.
(12) Bayly, C. I.; Cieplak, P.; Cornell, W. D.; Kollman, P. A. *J. Phys. Chem.* **1993**, *97*, 10269. It is difficult to compare results on the quality of the fits to the H bond potentials since the data presented are only at the minimum in the potential and not over the full range of H-bonding interactions. Note that there is an inaccuracy in the citation (h) of the molecular mechanics data in Table 16 of ref 10. The correct reference for this is ref 48 in this paper and ref 32 in their paper.
(13) Damewood, J. R., Jr.; Kumpf, R. A.; Mühlbauer, W. C. F.; Urban, J. J.; Eksterowicz, J. E. *Phys. Chem.* **1990**, *94*, 6619.
(14) Guo, H.; Karplus, M. *J. Phys. Chem.* **1992**, *96*, 7273.
(15) Mirkin, N. G.; Krimm, S. *J. Mol. Struct.* **1991**, *242*, 143.
(16) Dasgupta, S.; Goddard, W. A., III. *J. Chem. Phys.* **1989**, *90*, 7207.
(17) Dasgupta, S.; Yamasaki, T.; Goddard, W. A., III. *J. Phys. Chem.* **1996**, *104*, 2898.

$$E_{\tau x} = K_{\tau a} \cos\phi(\cos\theta_1 - \cos\theta_{1e})(\cos\theta_2 - \cos\theta_{2e}) + K_{\tau r}(R_1 - R_{1e})(R_2 - R_{2e}) \quad (9b)$$

where the coupling around central bond JK involves $K_{\tau a}$ between angles IJK and JKL and $K_{\tau r}$ between bonds IJ and KL. In order to provide a smooth dependence on the dihedral angle, we use the cos ϕ factor [1 for $\phi = 0$ (cis), -1 for $\phi = 180$ (trans), and 0 for $\phi = 90$].

The vdW term uses

$$E_{vdw} = D_v\left[\left(\frac{6}{\zeta - 6}\right)e^{\zeta(1-\rho)} - \left(\frac{\zeta}{\zeta - 6}\right)\rho^{-6}\right] \quad (10)$$

where $\rho = R_{IJ}/R_v$. Here D_v is the well depth, R_v is the distance at the minimum, and ζ is a dimensionless constant related to the stiffness of the inner wall.

$$E_Q = C_Q(e_1e_2/r)$$

where $C_Q = 332.0637$ converts units to give E_Q in kilocalories per mole when the charges are in electron units and distance is in angstroms.

The BH method systematically varies the FF parameters to obtain the closest fit to the *ab initio* normal modes, the experimental geometry, and the experimental frequencies. Since vibrational frequencies are a sensitive test of the accuracy of a FF, this ensures a vibrationally accurate FF. This method has been successfully used for many systems[18] and typically leads to a FF with vibrational frequencies accurate to about 10 cm^{-1}.

The most recent experimental studies (denoted SHT)[19] examined the 19 in-plane A′ modes for 9 isotopic species. In addition to the extensive analysis by MK of all four conformers for this molecule, an earlier *ab initio* calculation also assigned normal modes.[20] While there are some subtle differences in normal mode compositions between these two calculations and also with the experimentally refined FF of SHT, our HF/6-31G** normal modes agree quite well with the previous assignments. In the congested CH stretching region around 2800−3000 cm^{-1}, the order of modes differs for each calculation, but the differences are not significant. The only real disagreement is for the two lowest A″ frequencies. Like Balazs,[20] we find that the 1A″ mode involves torsion about the C−N bond with some amount of NH out-of-plane (oop) bending while the 2A″ modes is dominated by NH oop bending with a smaller torsion component. The calculations of MK have this reversed. We believe that this is probably a typographical error since their reported force constant for the C−N torsion is smaller than that for the NH oop bending.

Since all four conformers are so closely spaced in energy and the barriers to methyl rotations are negligibly small, all conformers are expected to coexist in the gas phase. Even in the hydrogen-bonded liquid phase, it is likely that all of the conformers coexist. Aside from MK, other calculations and experimental papers have not taken this into account. We chose to base our FF on fitting conformer **IV** using the scaled frequencies from MK (with the exceptions noted above). The results, Table 3, indicate that the match between the experimental and calculated frequencies is very good. The FF from fitting the vibrational frequencies leads to a barrier of 14.99 kcal/mol for the C−N partial double bond torsion, which compares favorably with the estimated barrier of 15 kcal/mol.[21]

Table 3. Normal Modes of *N*-Methylacetamide

mode[a]	amide	sym	exptl[b]	FF	HF
N−CH_3 τ		A″	52[c]	−106[e]	−44[e]
C−CH_3 τ		A″	139[c]	85	13
C−N τ + NH_{op} δ + CO op δ		A″	178[d]	177	171
CNC δ + CCN δ		A′	280	278	284
NH op δ		A″	454[d]	453	368
CCN δ + CO ip δ + (C)CH_3 ro		A′	450	451	457
CC ν + CO ip δ		A′	649	647	673
CO op δ + (C)CH_3 ro	**V**	A″	639	654	684
CN ν + (N)CH_3 ro + CNC δ		A′	861	861	948
(C)CH_3 ro + CC ν		A′	984	980	1090
(C)CH_3 ro + CO op δ		A″	1053	1005	1163
CN ν + (N)CH_3 ro		A′	1096	1101	1186
(N)CH_3 ro		A″	1117	1061	1258
(N)CH_3 ro + CN ν		A′	1179	1184	1305
NH ip δ + CO ip δ + CN ν	**III**	A′	1266	1262	1399
(C)CH_3 s δ + (C)CH_3 a δ	S[44]	A′	1378	1378	1540
(N)CH_3 s δ + (C)CH_3 a δ		A′	1423	1425	1595
(C)CH_3 a δ + (N)CH_3 a δ		A″	1429	1447	1600
(N)CH_3 a δ + (C)CH_3 a δ		A″	1441	1464	1611
(C)CH_3 a δ + (C)CH_3 s δ		A′	1441	1482	1615
(N)CH_3 a δ		A′	1469	1477	1644
NH ip δ + CN ν	**II**	A′	1512	1506	1703
CO ν + CCN δ	**I**	A′	1700	1700	1954
(N)CH_3 s ν		A′	2932	2930	3204
(C)CH_3 s ν		A′	2928	2929	3204
(N)CH_3 a ν		A″	2997	2974	3273
(C)CH_3 a ν		A′	3002	3015	3282
(N)CH_3 a ν		A′	2992	2990	3286
(C)CH_3 a ν		A″	2990	3006	3286
NH ν		A′	3510	3510	3929
error				20.47	121.75

[a] Abbreviations: τ for torsion, δ for bending, ip for in-plane, op for out-of-plane, ro for rocking, ν for stretching, a for antisymmetric, and s for symmetric. [b] These are experimental values (except as noted) from ref 15 which were assigned by comparison to scaled *ab initio* values for conformer **IV**. [c] These two frequencies are the theoretical values calculated by Balazs.[20] These are not used for parameter optimization as the methyls are essentially free rotors.[14] [d] These two A″ modes have different assignments in Balazs[20] and Mirkin and Krimm.[15] Our HF/6-31G** normal modes agree with the former, and consequently we used the scaled experimental frequencies from the former. [e] These two values are negative since this conformer is not the lowest energy rotamer for this methyl rotor in the HF and FF calculations.

2.3. Torsional Potentials. The single bond torsional potentials, C(amide)−C and N(amide)−C, are particularly important for nylon, and hence we calculated the full torsional potential by optimizing the geometry (using HF/6-31G**) at each point on the torsional curve. [Rigid rotation without geometry optimization leads to very bad contacts for particular values of the dihedrals, resulting in a poor description of the torsional potential.]

The barrier for rotation about the N(amide)−C bond, calculated for *N*-ethylacetamide, is shown in Figure 5b. The minimum is near 90° with a small trans barrier (0.54 kcal/mol). The cis barrier of 5.55 kcal/mol results from steric interactions. Between 90° and 180°, the potential is quite flat. The minimum in the N(amide)−C torsional potential near 90° apparently arises because the nitrogen π lone pair prefers to overlap the C−C bond (a weak anomeric effect). This leads to smaller repulsions arising from orthogonalization due to the Pauli principle than having it overlap the CH bonds.

In contrast, the C(amide)−C potential, calculated for *N*-methylpropionamide (Figure 5a) has its minimum near 163°, with a trans barrier of only 0.04 kcal/mol. The cis conformation is 1.60 kcal/mol above the trans conformation [there is a maximum (1.63 kcal/mol) near 30°].

(18) (a) Karasawa, N.; Dasgupta, S.; Goddard, W. A., III. *J. Phys. Chem.* **1991**, *95*, 2260. (b) Musgrave, C. B.; Dasgupta, S.; Goddard, W. A., III. *J. Phys. Chem.* **1995**, *99*, 13321. (c) Karasawa, N.; Goddard, W. A., III. *Macromolecules* **1992**, *25*, 7268. (d) Wendel, J. A.; Goddard, W. A., III. *J. Chem. Phys.* **1992**, *97*, 5048.

(19) Sugawara, Y.; Hirakawa, A.; Tsuboi, M. *J. Mol. Spectrosc.* **1984**, *108*, 206.

(20) Balazs, A. *J. Mol. Struct.*: *THEOCHEM* **1987**, *153*, 103.

(21) Dole, M.; Wunderlich, B. *Makromol. Chem.* **1959**, *34*, 29.

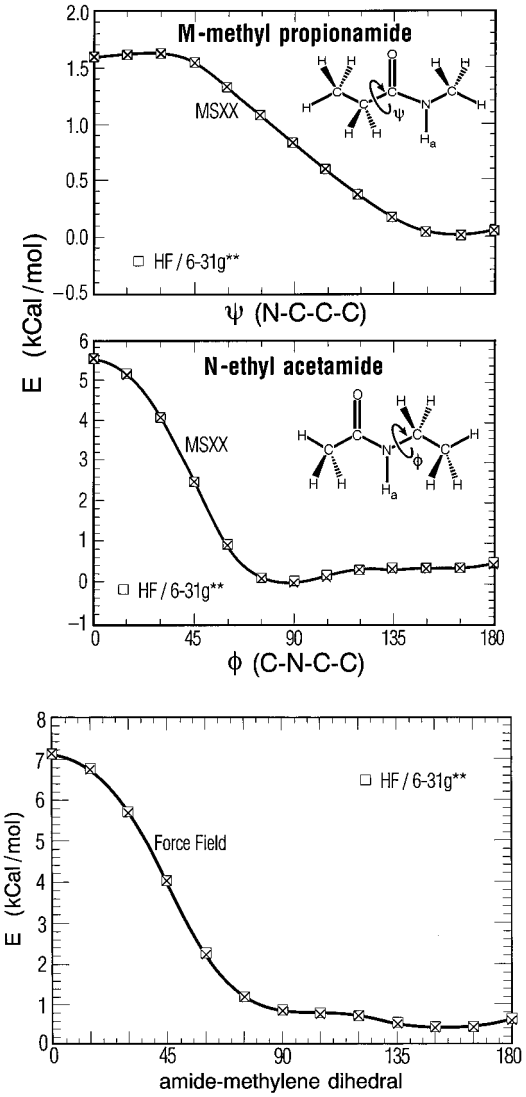

Figure 5. Torsional potentials: (a, top) the N(amide)−C(amide)−C−C dihedral in *N*-methylpropionamide, (b, middle) the C(amide)−N(amide)−C−C dihedral in *N*-ethylacetamide, (c, bottom) combination of both dihedrals. In each case the structure of the molecule was completely optimized for each value of the dihedral. Shown are the calculated values from HF/6-31G** (□) and from the FF (× inside □). A smooth line is drawn through the FF points to guide the eye.

The primary difference between the α and the γ forms of the even nylons is in these two dihedrals. Both dihedrals have the same value in order that the alkyl chains be all-trans. The α form has $\phi \approx 164$ to 168° while the γ form has $\phi \approx 126°$. This is expected from the theory. Figure 5c shows the two torsional curves added. Here we see a minimum at 160°, but the potential is quite flat all the way to 120°. Thus, distorting these two dihedrals from ∼160° in the α form to 126° in the γ form costs only 0.22 kcal/mol of energy.

In parametrizing the torsional potential about these two bonds, we use only the single heavy atom torsional barrier (C−N−C−C in *N*-ethylacetamide and N−C−C−C in *N*-methylpropionamide) while keeping the other barriers (like H−N−C−C, C−N−C−H, etc.) fixed at 0.0.

2.4. Charges. To derive the charges for the nylon simulations, we calculated potential derived charges (PDQs) for a series of small model amide molecules using the CHELPG scheme[22] in the Gaussian92 program, Figure 6. The PDQs show large deviations for various groups in similar positions in the different molecules, whereas the Mulliken populations show little variance. Indeed for crowded molecules PDQ charges sometimes lead to misleading results. Consequently we have averaged the PDQ charges from a series of molecules in such a way as to be consistent with the changes in Mulliken populations.

The final recommended charges are shown for the generic nylon backbone in Figure 6. We find a net charge of +0.2 on the methylene (or methyl) unit adjacent to the amide nitrogen, presumably because of the extra polarization due to the lone pair on the (electronegative) nitrogen. However, the methylene (or methyl) unit adjacent to the carbonyl C is neutral. On the basis of the averages of the amide charges for the series, we assign charges of −0.62 to O, 0.74 to C, −0.68 to N, and 0.32 to the amide H. From the hydrocarbon calculations,[23] we assign 0.14 to all methylene (or methyl) H atoms, with the exception of the methylene adjacent to the N. From charge neutrality, all methylene C atoms are assigned equal and opposite charges (−0.28 or −0.42). For the methylene adjacent to the amide N the C has a charge of −0.06 and the H has a charge of 0.13, leading to a net transfer of 0.2 electron unit to the amide group. The full FFs for the nylon simulations are reported in Table 4.

3. Nylon Polymers

3.1. Types of Nylon. The naming scheme for unsubstituted nylon is as follows. If polymerized from the monoacid [NH_2−$(CH_2)_{n-1}$−C(O)(OH)] to form (1), it is designated as nylon-*n*. If made from the condensation of the diamine [H_2N−$(CH_2)_m$−NH_2] and the diacid [C(O)(OH)−$(CH_2)_{n-2}$−C(O)(OH)] to form (2), it is denoted as nylon-*m*,*n*. Commercially, the most important nylons are nylon-6,6 and nylon-6, which are used in carpet fibers and textiles.

3.2. Crystal Structures. The crystal structures observed for nylons fall into two categories:[24] (1) α and β phases (this includes the even nylons-4 and -6, even−even nylons-6,6 and -6,10, and odd nylons-7 and -11), (2) γ phase (this includes the even nylons from -8 up and the even−odd, odd−even, and odd−odd nylons). The stable α phase (category 1) consists of *planar sheets of hydrogen-bonded chains* with sheets stacked upon one another and displaced along the chain direction by a fixed amount, Figure 1a. The β phase is not distinct, probably involving a small modification of the α phase. There is no definitive crystal structure, and this form is not of practical interest. The γ phase (category 2) has pleated sheets of the methylene units with hydrogen bonding *between* sheets rather than *within* sheets,[25] Figure 1b.

The principal structural difference between α and γ forms is that the amide-to-methylene dihedrals are near trans (164−168°) in α and nearly perpendicular to the peptide plane (∼126°) in γ. With axial tension the γ form can usually be converted to the α form.[26−28]

Nylon-4 and -6 are unusual because they are observed to crystallize in both the α and γ phases. For nylon-6 the γ phase is less stable and can be transformed to the α phase by various treatments, including pressure.

(22) (a) Chirlian, L. E.; Francl, M. M. *J. Comput. Chem.* **1987**, *8*, 894. (b) Breneman, C. M.; Wiberg, K. B. *J. Comput. Chem.* **1990**, *11*, 361.

(23) Karasawa, N.; Dasgupta, S.; Goddard, W. A., III. *J. Phy. Chem.* **1990**, *95*, 2260.

(24) Kohan, M. I. *Nylon Plastics*; Wiley-Interscience, John Wiley and Sons: New York, 1973.

(25) In the α phase, the sheets are easy to define since the methylene spacers are nearly coplanar with the amides, which are H-bonded to amides from the adjacent chains. In the γ phase the methylene spacers are twisted with respect to the amide planes; thus, we refer to the methylene planes as the sheets and consider the amides as H-bonded to chains in adjacent sheets rather than within the same sheet.

(26) Kyotani, M.; Mitsuhashi, S. *J. Polym. Sci., A-2* **1972**, *10*, 1497.

(27) Abu-isa, I. *J. Polym. Sci., A-1* **1971**, *9*, 199.

(28) Hiramatsu, N.; Hirakawa, S. *Polym. J.* **1982**, *14*, 165.

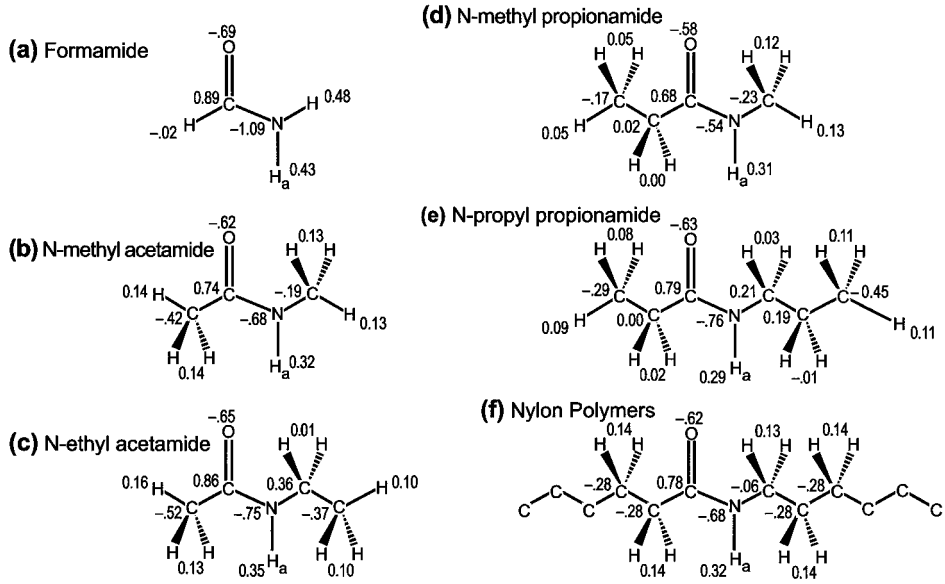

Figure 6. Charges for various amide models and nylon polymers.

Fredericks et al. reported[29] the crystal structure of the α phase of nylon-4. They also reported studies on what they called the β and δ polymorphs, but these were distinctive from the γ phase. The β polymorph is converted to the α phase in air by heating followed by immersion in water. The δ polymorph is formed by rapid quenching of extruded nylon-4 against chilled rods, but is metastable and completely converted to the α phase by orientation.

Using the MSXX FF, we determined the stable crystal structures for most nylons. Table 5 shows the predicted structures at 0 K. With increasing temperature, the chain axis direction contracts because increased thermal motion distorts the dihedrals from all-trans, whereas directions perpendicular to the chain axis expand.

3.3. Nylon-6 α. There is substantial confusion regarding the structure of nylon-6 α. The earliest crystal structure reported[30] had some incorrect atomic coordinates which were subsequently rectified.[31] A later study[32] found slightly different dimensions, particularly along the chain axis, but the most recent studies[33−34] find dimensions similar to those of the earlier work.[30] The fiber diffraction pattern does not yield enough data to uniquely determine the structure, and the actual coordinates were deduced from model building. Thus, the setting angle of the chains, the sense of successive sheets, and their displacements along the chain axis were determined by trial and error calculations of diffraction intensity from various models.[30] For nylon-6 α, the data cannot distinguish between the $P2_1$ and $P2_1/c$ space groups.

We calculated the crystal packing energies of the $P2_1$ and the $P2_1/c$ structures and found the $P2_1$ packing is energetically better by about 0.60 kcal/mol per amide. The valence interactions slightly favor $P2_1/c$ (by 0.09 kcal/mol per amide) but nonbonded terms (including the hydrogen bond energy) favor $P2_1$ by 0.69 kcal/mol per amide.

The minimized $P2_1$ structure shows a significant structural feature not expected from previous analyses of the crystal structure. The plane of the methylene units is tilted 17° from the plane of the amides. This is expected from the N−C−C−C and C−N−C−C dihedral potentials, Figure 5. Simultaneous twisting of both bonds leads to a minimum at 160° with an energy 0.18 kcal/mol below planar. Indeed twisting the methylene chain by 50° from the plane increases the energy by only 0.2 kcal/mol. Such twisting leads to a slight *contraction* of the chain repeat distance by 0.067 Å.

Table 5 shows the optimum cell dimension along the chain axis to be 17.602 Å (0 K), significantly larger than the experimental values[35] of 17.24−17.4 Å reported for $T = 423-133$ K. The observed negative expansivity and larger value at 0 K is expected from chain flexing.

Two models have been proposed for the chain contraction: (i) Natta and Corradini[36] suggested that the chains twist at the amide groups while (ii) Ito[37] proposed that the twisting is at the methylene groups. The X-ray data did not allow definite conclusions as to which model is correct in the 123−423 K range. Our calculations clearly indicate that *the primary twisting occurs at the amide groups and is present for all* α *phase nylons.* Sakurada and Kaji[38] speculate that nylon-6,10 assumes a strictly planar structure; however, we find that nylon-6,10 twists to 168° just as the others, Table 5.

Perpendicular to the chain axis, the hydrogen-bonded direction is longer ($A = 9.587$ Å) than the vdW direction perpendicular to the sheets ($C = 7.760$ Å). This is because the packing of the methylene units on adjacent sheets is staggered, whereas they are more eclipsed between the H-bonded chains in the same sheet (because of the hydrogen-bonding forces).

The hydrogen-bonding distance of N:::O is 2.96−2.99 Å (Table 6) is in good agreement with the 2.98 Å reported by Malta *et al.*,[32] but longer than the 2.81 Å reported by Holmes *et al.*[30] The H:::O distance of 2.00 Å compares to the value of 1.8 Å in ice.

The shortest nonbonded distances between alkyl H atoms on different chains is 2.14 Å which is considerably shorter than the 2.45 Å in polyethylene. This contrasts with the γ structure where the shortest distances are 2.47 Å. This shows that in the α form hydrogen bonding squeezes the chains together to cause bad $CH_2\cdots CH_2$ interactions.

(29) Fredericks, R. J.; Doyne, T. H.; Sprague, R. S. *J. Polym. Sci., A-2* **1966**, *4*, 899, 913.
(30) Holmes, D. R.; Bunn, C. W.; Smith, D. J. *J. Polym. Sci.* **1955**, *17*, 159.
(31) Simon, P.; Argay, Gy. *J. Polym. Sci., Polym. Phys. Ed.* **1978**, *16*, 935.
(32) Malta, V.; Cojazzi, G.; Fichera, A.; Ajo, D.; Zanetti, R. *Eur. Polym. J.* **1979**, *15*, 765.
(33) Salem, D. R.; Weigmann, H.-D. *Polym. Commun.* **1989**, *30*, 336.
(34) Murthy, N. S.; Minor, H. *Polym. Commun.* **1991**, *32*, 297.
(35) Miyasaka, K.; et al. *J. Polym. Sci., Polym. Phys. Ed.* **1980**, *18*, 1047.
(36) Natta, G.; Corradini, P. *Nuovo Cimento Suppl.* **1960**, *15*, 9.
(37) Ito, T. *Jpn. J. Appl. Phys.* **1976**, *15*, 2295.
(38) Sakurada, I.; Kaji, K. *J. Polym. Sci., C* **1970**, *31*, 57.

Table 4. Force field Parameters for Nylons[a]

bonds (eq 5a,b)	K_b	R_b	D_b
N_2-H	975.01	1.008	
C_2-O	1221.20	1.210	
C_2-N_2	685.09	1.357	
C_2-C_3	757.91	1.535	
N_2-C_3	940.93	1.441	
C_3-C_3	917.22	1.483	85.8
C_3-H	726.71	1.076	95.1

angles (eqs 6 and 9a)	K_θ	θ_e	$K_{r_1\theta}$	$K_{r_2\theta}$	$K_{r_1r_2}$
$H-N_2-C_2$	113.25	109.48	16.21	−12.93	0.00
$H-N_2-C_3$	76.02	98.43	−47.87	−25.21	0.00
$C_2-N_2-C_3$	259.05	112.11	−18.68	30.44	22.38
$O-C_2-N_2$	204.53	120.09	−54.04	−141.99	4.11
$O-C_2-C_3$	164.79	122.18	−155.43	−0.66	22.20
$N_2-C_2-C_3$	47.60	119.24	24.77	4.59	95.25
$N_2-C_3-C_3$	82.82	121.68	−53.52	−53.52	26.55
N_2-C_3-H	122.15	104.12	−42.48	−44.28	0.00
$H-C_3-C_3$	63.98	118.21	−28.08	−35.68	12.66
$H-C_3-H$	54.12	119.64	−23.01	−23.01	3.73
$C_3-C_3-C_3$	82.82	121.68	−53.52	−53.52	26.55
C_2-C_3-H	100.48	106.48	−31.15	3.24	0.00
$C_2-C_3-C_3$	82.82	121.68	−53.52	−53.52	26.55

inversions (eq 8)	K_ϕ	ψ_i
$C_2-X-X-X$	73.95	0.00
$N_2-X-X-X$	20.68	0.00

torsions (eq 7)	V_0	V_1	V_2	V_3	V_4	V_5	V_6
$H-C_3-C_3-H$	2.58	0.00	0.00	2.58	0.00	0.00	0.00
$H-C_3-C_3-C_3$	3.08	0.00	0.00	3.08	0.00	0.00	0.00
$C_3-C_3-C_3-C_3$	2.85	0.00	0.00	2.85	0.00	0.00	0.00
$N_2-C_2-C_3-C_3$	−0.67	12.31	−0.97	−2.34	0.63	−0.10	0.07
$N_2-C_2-C_3-H$	0.00	0.00	0.00	0.00	0.00	0.00	0.00
$O_2-C_2-C_3-H$	0.00	0.00	0.00	0.00	0.00	0.00	0.00
$O_2-C_2-C_3-C_3$	0.00	0.00	0.00	0.00	0.00	0.00	0.00
$C_2-N_2-C_3-C_3$	−2.66	−0.78	3.67	−0.26	0.64	−0.14	0.09
$H-N_2-C_3-H$	0.00	0.00	0.00	0.00	0.00	0.00	0.00
$C_2-N_2-C_3-H$	0.00	0.00	0.00	0.00	0.00	0.00	0.00
$H-N_2-C_3-C_3$	0.00	0.00	0.00	0.00	0.00	0.00	0.00
$H-N_2-C_2-C_3$	12.38	0.00	−7.88	0.00	0.00	0.00	0.00
$H-N_2-C_2-O_2$	12.38	0.00	−8.90	0.00	0.00	0.00	0.00
$C_3-N_2-C32-C_3$	12.38	0.00	−12.88	0.00	0.00	0.00	0.00
$C_3-N_2-C_2-O_2$	12.38	0.00	−10.25	0.00	0.00	0.00	0.00
$C_2-C_3-C_3-H$	0.55	0.00	0.00	0.55	0.00	0.00	0.00
$N_2-C_3-C_3-H$	3.08	0.00	0.00	3.08	0.00	0.00	0.00
$C_2-C_3-C_3-C_3$	2.85	0.00	0.00	2.85	0.00	0.00	0.00
$N_2-C_3-C_3-C_3$	2.85	0.00	0.00	2.85	0.00	0.00	0.00

torsion cross terms (eq 9b)	$K_{\tau a}$	$K_{\tau\tau}$
$H-N_2-C_2-C_3$	−5.06	0.00
$H-N_2-C_2-O_2$	0.33	0.00
$C_3-N_2-C_2-C_3$	−48.83	40.43
$C_3-N_2-C_2-O_2$	−23.10	1.48
$H-C_3-C_3-H$	−17.73	0.00
$H-C_3-C_3-C_3$	−16.40	0.00
$C_3-C_3-C_3-C_3$	−21.59	0.00

van der Waals (eq 10)	R_v	D_v	ζ
H	3.1665	0.0200	12.0000
C_3	3.8410	0.0792	13.0000
C_2	3.8410	0.0792	13.0000
N_2	3.6621	0.0774	13.8430
O_2	3.4046	0.0957	13.4820
O_2:::H	3.0170	0.0280	12.0000

[a] The charges are given in Figure 6. Units: kcal/mol for energy, Å for distances, deg for structure angles, rad for force constant angles.

While nylon-6 is most stable in the α form, a γ form has also been observed. We calculated the minimized crystal structure and energetics of the γ form, Tables 5−7. After correcting for ZPE, the α form is more stable than the γ form by 0.304 kcal/mol per amide unit. However, since the volume per chain is smaller for the γ form, the cohesive energy density is slightly larger than that of the α form. The chain axis for γ is 0.33 Å shorter than for α since two dihedrals (126.5° and 126.6°) are significantly smaller than the 165° for α. While the N:::O = 2.98 Å distance of γ is similar to the value for the α form, the H:::O distance is 0.025 Å longer. This trend is present in all even-*n* α and γ forms that we have calculated, Table 5.

Similar trends are observed in other nylons. One must be cautious with most crystallographic determinations since single-crystal data are rare and the fiber diffraction patterns indicate the presence of amorphous material. For all nylons the calculated chain axis dimension at 0 K is 0.3−0.4 Å larger than the room temperature crystallographic value. This is explained in terms of increased torsional motions about the chain axis with increasing temperature, which should decrease the average chain axis dimensions.

In contrast, the axes perpendicular to the chains are dominated by vdW packing between adjacent sheets in the α form and between adjacent chains in the γ form. Here the calculated structures at 0 K are smaller than the room temperature measurements. The increase in these dimensions with increasing temperature is expected because of the asymmetry in vdW interactions.

The lattice parameter in the hydrogen-bonding direction exhibits a curious behavior. For all γ phases and for the α form of nylon-4 and -6, the calculated values at 0 K are *larger* than the measured values at room temperature, while the trend reverses for α nylon-*n* with $n \geq 7$. Thus, increasing temperature leads to better hydrogen bonds in the γ forms and in the α forms for nylon-4 and -6. This trend coincides with the stability of the α form versus the γ form in the nylons.

3.4. Stability of α Form vs γ Form. One puzzle about nylon is the change in relative stabilities of the α form versus the γ form, which for the even nylons reverses above nylon-6. In the α form the shortest H:::H nonbonded distances are 2.293 Å in 4 α, 2.140 Å in 6 α, 2.231 Å in 8 α, 2.247 Å in 7 α, 2.318 Å in 6,6 α, and 2.302 Å in 6,10 α. These are significantly shorter than those in the γ form: 2.464 Å in 4 γ, 2.466 Å in 6 γ, 2.469 Å in 8γ, and 2.468 Å in 10 γ. The optimum packing of the methylene units occurs in polyethylene,[23] where the minimum distance is 2.447 Å. Thus, the packing of the methylene units is optimum in the γ form and too short in the α form. These short distances in α are caused by the short H:::O distances required for the best hydrogen bonds. These competing effects determine the thermal stabilities of the two forms. As the number of methylene units increases, the more efficient packing of the CH_2 groups compensates for the slightly poorer hydrogen bonds in the γ form, making this the more stable form.

3.5. Elastic Constants. Young's Modulus. If σ_I and e_J are the stress and strain in the *I* and *J* directions (*I*, *J* = 1, 2, ..., 6 denotes *xx*, *yy*, *zz*, *yz*, *zx*, and *xy*), then they are related to each other by Hooke's law for small deformations:

$$\sigma_I = C_{IJ} e_J \tag{11}$$

$$e_J = S_{JI} \sigma_I \tag{12}$$

where C_{IJ} are the elastic stiffness constants and S_{IJ} are the compliance constants. The bulk modulus β is defined by

$$\beta^{-1} = \sum_{I,J=1}^{3} S_{IJ} \tag{13}$$

and Young's modulus in the chain direction is defined by

Table 5. Comparison of Calculated (0 K) and Experimental (298 K) Crystal Parameters for Various Nylon Crystals

		4		6			8				
property	description	α	γ	α	γ	6,6 α	α	γ	7 α	6,10 α	10 γ
A	calcd	9.634	9.898	9.587	4.931	9.737	9.549	4.912	9.629	4.752	4.900
	exptl	9.29		9.56	4.78	9.8	9.8	4.77	9.8	4.95	4.78
B	calcd	12.510	12.165	17.602	17.267	10.272	7.820	8.816	9.741	4.827	8.825
	exptl	12.24		17.24	16.88	10.8	8.3	9.54	9.8	5.4	9.56
C	calcd	7.821	8.781	7.760	8.810	17.620	22.657	22.360	10.099	22.705	27.453
	exptl	7.97		8.02	9.33	17.2	22.4	21.9	10.0	22.4	26.9
α	calcd	90.0	90.0	90.0	90.0	50.1	90.0	90.0	55.3	56.1	90.0
	exptl	90.0		90.0	90.0	48.5	90.0	90.0	56.0	49.0	90.0
β	calcd	113.4	126.9	69.0	126.8	83.9	90.0	90.0	89.0	87.7	90.0
	exptl	114.5		67.5	121.0	77.0	90.0	90.0	90.0	76.5	90.0
γ	calcd	90.0	90.0	90.0	90.0	67.0	111.0	126.67	69.1	69.4	126.6
	exptl	90.0		90.0	90.0	63.5	115.0	120.0	69.0	63.5	120.0
density	calcd	1.307	1.337	1.229	1.252	1.234	1.188	1.208	1.197	1.182	1.179
	exptl	1.37		1.16	1.14	1.24	1.08	1.07	1.19	1.157	1.056
ref		29		30	45	46	47	43	50,51	46	43

Table 6. Geometric Properties

	4		6			8				
property	α	γ	α	γ	6,6 α	α	γ	7 α	6,10 α	10 γ
H···H[a]	2.293	2.464	2.140	2.466	2.318	2.231	2.469	2.247	2.302	2.468
NH:::OC[b]	2.022	2.046	2.000	2.025	1.999	1.997	2.013	2.070	1.991	2.002
N:::O	2.990	3.027	2.995	3.009	2.975	2.976	2.994	2.997	2.941	2.985
angle N−H:::O	162.5	167.9	161.0	168.5	166.1	159.8	168.2	151.2	159.3	168.1
angle C═O:::H	158.1	166.4	158.6	167.1	164.4	157.7	166.8	145.6	157.8	166.7
ψ[(NH)−(CO)−(CH_2)−(CH_2)]	165.6	126.7	168.3	126.5	163.2	168.7	126.6	169.1	168.4	126.7
ϕ[(OC)−(NH)−(CH_2)−(CH_2)]	163.5	126.0	166.3	125.6	163.9	166.1	125.3	166.5	167.5	125.1

[a] Shortest nonbonded distance between H atoms on CH_2 groups of different chains. In polyethylene, it is 2.447 Å. [b] Hydrogen-bonded distance.

$$E_c = \sigma_c/e_c \quad (14)$$

The Young's modulus can be calculated by using the analytic first derivatives of the energy with respect to cell parameters. The calculated Young's moduli are reported in Table 7. This should be regarded as the ultimate modulus, that is, the longitudinal crystal modulus for a perfectly aligned, fully crystalline polymer. The calculated elastic stiffness constants C_{ij} are reported in Table 2S (Supporting Information).

Young's modulus is one of the most important properties of nylon. However, it has been difficult to measure these values. The most reliable experimental moduli are obtained directly from spectroscopy using neutron and Raman scattering.[39,40] The spectroscopic measurements provide data on the phonon dispersion, which leads directly to Young's modulus. Unfortunately, such values have not yet been reported for nylons. For nylon the moduli have been estimated from X-ray experiments in which the crystalline strain is determined by monitoring the change in the *d* spacing of a plane perpendicular to the polymer chain axis under application of macroscopic stress to the ends of an oriented polymer. This assumes that the stress is distributed uniformly through the material, including the amorphous regions. In general values determined from X-ray analysis are 30−40% lower than from direct spectroscopy.[41,42] In contrast the MSXX FF leads to moduli within 5% of the direct experiment.[23] The X-ray determined experimental value of 168 GPa[38] for nylon-6 is 29% lower than the calculated value of 235.3 GPa.

An indication of the error in using the X-ray technique is the dependence upon which the diffraction line is used. Sakurada and Kaji report[38] moduli of 25, 55, and 168 GPa using the [0,2,0], [0,4,0], and [0,14,0] reflections for nylon-6, and they report 61 and 176 GPa using the [0,1,5] and [1,3,14] reflections for nylon-66. Further confusing the interpretation of such studies, the fiber identity periods for nylons calculated from the various meridional reflections disagree with each other.[41] In light of recent redetermination[42] of longitudinal crystal moduli using spectroscopic methods, we believe that our calculated results are significantly more reliable than those determined from X-ray experiments.

Young's moduli of the α form is systematically higher than for γ. This is expected from the more extended structure of the α form. With increasing methylene units the modulus increases monotonically for the γ form of even nylons and decreases monotonically for the α form. The odd and the even−even nylons display much higher moduli, with nylon-7 being the highest calculated.

4. Summary

We used *ab initio* wave functions to calculate the MSXX FF for nylons. With this new nylon FF, we calculated the crystal structures of a series of nylon polymers. We find that the even nylons-4 and -6 exist in the α form, while the γ form is thermodynamically more stable for even nylons-8 and above.

(39) Rabolt, J. F.; Fanconi, B. *J. Polym. Sci., Polym. Lett. Ed.* **1977**, *15*, 121.
(40) Rabolt, J. F.; Fanconi, B. *Polymer* **1977**, *18*, 1258.
(41) Wallner, L. G. *Monatsh. Chem.* **1948**, *79*, 86.
(42) Fanconi, B.; Rabolt, J. F. *J. Polym. Sci., Polym. Phys. Ed.* **1985**, *23*, 1201.
(43) Cojazzi, G.; Fichera, A.; Malta, V.; Zannetti, R. *Makromol. Chem.* **1978**, *179*, 509.
(44) Wang, Y.; Purrello, R.; Jordan, T.; Spiro, T. G. *J. Am. Chem. Soc.* **1991**, *113*, 6359.
(45) Arimoto, H. *J. Polym. Sci., A* **1964**, *2*, 2283.
(46) Bunn, C. W.; Garner, E. V. *Proc. R. Soc. London* **1947**, *A189*, 39.
(47) Vogelsong, D. C.; Pearce, E. M. *J. Polym. Sci.* **1960**, *45*, 546.
(48) Gould, I. R.; Kollman, P. A. *J. Am. Chem. Soc.* **1994**, *116*, 2493.
(49) Harmony, M. D.; Laurie, V. W.; Kuczkowski, R. L.; Schwendeman, R. H.; Ramsey, D. A.; Lovas, F. J.; Lafferty, W. J.; Maki, A. G. *J. Phys. Chem. Ref. Data* **1979**, *8*, 619.
(50) Slichter, W. P. *J. Polym. Sci.* **1959**, *36*, 259.
(51) Hasegawa, R. K.; Kimoto, K.; Chatani, Y.; Tadokoro, H.; Sekiguchi, H. *Discussion Meeting of the Society of Polymer Science, Japan, Tokyo, Preprint 713*, 1974.

Table 7. Energy Properties of Nylon Polymers[f]

		4		6			8				
property	description	α	γ	α	γ	6,6 α	α	γ	7 α	6,10 α	10 γ
energy	crystal	−19.432	−19.160	−11.993	−11.670	−12.237	−4.338	−4.441	−7.198	−4.435	2.942
	sngl chn[a]	−3.095	−3.095	8.481	8.481	8.395	20.300	20.300	14.926	20.352	32.190
ZPE[b]	crystal	68.261	68.477	102.267	102.444	102.217	136.187	136.418	119.103	135.919	170.351
	sngl chn[a]	67.269	67.269	101.190	101.190	101.140	134.603	134.603	117.653	134.489	168.385
lattice E[c]		15.345	14.857	19.397	18.897	19.555	23.054	23.083	20.674	23.3575	27.282
volume		108.126	105.710	152.842	150.111	152.289	197.431	194.136	176.494	198.309	238.325
CED[d]		0.14192	0.14054	0.12691	0.12589	0.12841	0.11677	0.11890	0.11714	0.11778	0.11447
Young's modulus[e]		242.92	96.34	235.29	131.97	261.60	199.89	154.94	288.70	232.207	172.367

[a] For the isolated chain, the cell dimensions perpendicular to the chain axis were increased to 50 Å and the structure was reminimized. [b] The zero point energy (ZPE) is calculated using $3^3 = 27$ points in the Brillouin zone. [c] The lattice energy is after correction for ZPE. It is calculated by first taking the difference between the total energy per amide of the packed nylon crystal and the single chain (50 Å cell size for the nonchain directions) and then adding the difference of the zero point energies of the two. For example, for nylon-4 α, the difference of the energy is $-3.095 - (-19.432) = 16.337$ kcal/mol. The difference in ZPEs for the two is $67.269 - 68.261 = -0.992$ kcal/mol. Adding these two differences gives the lattice energy as $16.337 - 0.992 = 15.345$ kcal/mol. [d] The cohesive energy density (CED) is the lattice energy divided by the volume per amide unit [units of (kcal/mol)/Å^3]. [e] GPa. [f] The energies (kcal/mol) are calculated from the total energy of the optimized crystal. All energies are normalized per amide.

This results from the interplay of better H bonds in α at the expense of poorer methylene packing. Thus, γ is favored for larger n.

The cell dimensions calculated at 0 K are compatible with those measured at room temperature as deduced from expansivity measurements. In nylon-6, we find that the $P2_1$ packing is better than the $P2_1/c$ packing (resolving an experimental uncertainty).

The calculated Young's moduli provide the first reliable trends in these values and are expected to be more accurate than the values measured experimentally using the X-ray technique. Other elastic constants are also reported.

Acknowledgment. The research was funded by AlliedSignal Inc. and by NSF (Grants CHE 94-13930, CHE 95-22179, and GCAG-ASC 92-17368). The facilities of the MSC are also supported by DOE-BCTR, Asahi Chemical, Asahi Glass, BP Chemical, Chevron Petroleum Technology Co., BF Goodrich, Vestar, Hughes Research Laboratories, Teijin Ltd., and the Beckman Institute. Some of these calculations were carried out at the NSF Pittsburgh Supercomputer Center and on the JPL Cray system.

Supporting Information Available: Tables giving the geometries and energies of *N*-methylacetamide conformers and elastic stiffness constants of crystalline nylon polymers (2 pages). See any current masthead page for ordering and Internet access instructions.

JA944125D